

A Theoretical Study of the Radiationless Decay Mechanism of Cyclic Alkenes in the Lowest Triplet State

Markus Woeller, Stefan Grimme, and Sigrid D. Peyerimhoff*

Institut für Physikalische und Theoretische Chemie der Universität Bonn, Wegelerstrasse 12, 53115 Bonn, FRG

David Danovich, Michael Filatov, and Sason Shaik

Department of Chemistry and the Lise-Meitner-Minerva Center for Computational Quantum Chemistry, The Hebrew University, IL-91904 Jerusalem, Israel

Received: January 27, 2000; In Final Form: March 21, 2000

The radiationless decay mechanisms of cyclic alkenes C_nH_{2n-2} ($n = 4, 5, 6$), norbornene, their phenyl derivatives, and styrene in their lowest triplet state have been investigated by unrestricted density functional, *ab initio* CASSCF, and MRD-CI calculations. The potential energy surfaces of the ground (S_0) and lowest triplet state (T_1) have been explored along double bond twisting and anti pyramidalization reaction pathways to explain the experimentally observed inverse proportionality between ring size and triplet-state lifetime. The calculations for the transition probabilities between T_1 and S_0 states are based on Fermi's golden rule including spin-orbit coupling (SOC) constants. According to the older "free-rotor model", the hindered twist around the double bond in small ring alkenes has been assumed so far to be the main factor determining the T_1 -state lifetimes. All computational results show, however, that only a combined reaction coordinate of anti pyramidalization and twisting at the double bond provides a low-energy pathway which reproduces the experimentally observed transition probabilities. For the relative transition rates, the different Franck-Condon (FC) factors in the series of compounds are found to be much more important than the SOC constants (FC-controlled mechanism). On the basis of the theoretical model, the effect of substitution of vinylic hydrogen atoms by phenyl groups is discussed.

1. Introduction

The radiationless decay of electronic excitation energy often controls the efficiency of important photochemical processes.¹ Especially the spin-forbidden radiationless transition from the first excited triplet state (T_1) to the singlet ground state (S_0) is very efficient in organic molecules with a carbon-carbon double bond and thus plays an important role in a wide variety of organic photoreactions.¹ Acyclic alkenes, which usually have a planar double bond geometry in their ground state, are expected to reach a perpendicular twisted structure in their relaxed T_1 state.^{1,2} In a simple picture this excited state arises by promoting an electron from the highest occupied π orbital to its antibonding π^* counterpart. The reduced Coulomb repulsion between the electrons that is no longer offset by any π -bonding favors a twisted triplet geometry with two perpendicular methylenic groups. From experiments³⁻⁵ and *ab initio* calculations^{6,7} a perpendicular twisted structure is well known to provide an energetic near degeneracy between S_0 and T_1 states for ethene. This twisted T_1 minimum constitutes a funnel geometry for spin inversion, and it was believed that such a geometry is responsible for an efficient $T_1 \rightarrow S_0$ transition also in other alkenes. Mainly induced by spin-orbit (SO) interaction the triplet excited alkene changes the spin state of one of the excited electrons to become an isoenergetic rovibrational excited ground-state molecule. This intersystem-crossing (ISC) mechanism results for several alkenes in the well-known cis-trans isomerization.¹

Cyclic alkenes should be hindered in their ability to twist to a perpendicular funnel geometry. The free-rotor model⁸ assumes that the high ring strain of small cyclic alkenes prevents efficient

radiationless decay. The locked double bond of rigid molecules is supposed to effect a planar triplet minimum geometry that causes a large barrier on the T_1 surface between the minimum and the perpendicular twisted geometry and provides a sizeable energy gap between the T_1 and S_0 states. According to Siebrand,⁹ an increased energy gap will result in an increase of the triplet-state lifetime. This model of forced planarity was used to explain the experimentally observed inverse proportionality between T_1 state lifetimes and ring size^{4,8} for phenyl-substituted cyclic alkenes.

In addition to these energetic arguments (ring strain) of the free-rotor model, the physics of the spin-forbidden $S_0 \rightarrow T_1$ transition is well known to also be determined by vibronic resonance and spin-orbit coupling (SOC) between the two states.^{1,9,10} A measure for resonance of vibronic states is the Franck-Condon factor (FCF) between the triplet vibronic ground state (v_0') and an isoenergetically lying highly excited singlet state ($v_j, j \gg 0$). According to Fermi's golden rule, the $T_1(v_0') \rightarrow S_0(v_j)$ transition rate depends quadratically on the spin-orbit coupling matrix element with the spin-orbit operator H_{SO} between the two states and on the ground-state density of rovibronic states ρ_{S_0} with energy comparable to that of the T_1 -(v_0') state:

$$k_{T_1 \rightarrow S_0} = (2\pi/\hbar) |\langle \chi_{T_1} | \langle \phi_{T_1} | H_{SO} | \phi_{S_0} \rangle \chi_{S_0} \rangle|^2 \rho_{S_0} \quad (1)$$

ϕ represents the electronic and χ the vibrational wave functions. It is not a priori clear whether FC or SO factors will be the dominant part of the transition rate, and thus, theoretical considerations are required.

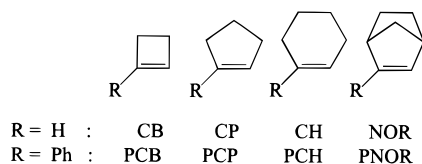


Figure 1. Systems investigated and their abbreviations.

Rowland and Salem¹¹ derived simple rules to estimate the magnitude of spin-orbit interaction for 1,2-biradicaloids such as cycloalkenes in the T_1 state. Large SOC will be favored (i) by nonparallel vinylic p_z atomic orbitals due to different orbital angular momentum and (ii) by an ionic contribution of the singlet wave function to enhance a spatial redistribution of electrons with the purely covalent triplet state. However, even for the simplest compound ethene with a very short lifetime of about 10 ns² for the T_1 state, a quantitative description of the ISC using the double bond twist path alone is problematic. At the funnel geometry (90° twist) the singlet wave function is purely covalent, and therefore SOC between T_1 and S_0 is negligible (the FCFs are also very small).^{7,12} To explain the experimentally observed efficient transition, distortions away from a perpendicular twisted T_1 geometry must be considered.^{12,13} Already Walsh¹⁴ proposed a pyramidal arrangement of the twisted methylene groups in the $\pi\pi^*$ states which have recently been proved by a quantum-dynamical study¹⁵ to be important for the $S_1 \rightarrow S_0$ decay of ethene. Higher SOC values for pyramidalized geometries found by *ab initio* calculations of Caldwell et al.¹² and Danovich et al.¹⁶ seem to corroborate this idea.

The quantitative description of $T_1 \rightarrow S_0$ radiationless deactivation of cyclic alkenes is even more complicated due to the expected absence of a clear funnel geometry. The qualitative predictions of the free-rotor model have several exceptions, e.g., the T_1 -state lifetime of the bicyclic alkene norbornene (NOR). Although having a quite rigid double bond geometry in the five-membered ring (23.6 kcal/mol ground-state strain energy¹⁷), norbornene shows an unexpected short triplet lifetime (250 ns¹⁸) which cannot be explained in the framework of a twist mechanism.¹⁹

In the present paper we consider the $T_1 \rightarrow S_0$ decay mechanism of 1-phenylcycloalkenes with various ring sizes (see Figure 1) which have been used as the experimental basis of the free-rotor model.^{5,8} In particular we study the styrene derivatives 1-phenylcyclobutene (PCB), 1-phenylcyclopentene (PCP), and 1-phenylcyclohexene (PCH) as well as the unsubstituted parent compounds cyclobutene (CB), cyclopentene (CP), and cyclohexene (CH). The phenylalkenes have been studied with a wide variety of experimental methods in the last 20 years such as time-resolved photoacoustic calorimetry,⁴ laser-flash photolysis,^{5,20} oxygen and heavy-atom perturbation,⁴ and nanosecond flash kinetic absorption spectroscopy.² All experiments show a correlation between triplet lifetime and ring strain. Adding a CH_2 group to the ring reduces the ground-state strain energy by more than 50%^{17,21} and decreases the T_1 lifetime by more than a factor of 100 ($\tau_{T_1}(\text{PCB}) = 4$ ms, $\tau_{T_1}(\text{PCP}) = 15$ μs , and $\tau_{T_1}(\text{PCH}) = 56$ ns).^{2,4,5} The free-rotor model explains this trend by the amount of possible twist according to Dreiding models² (e.g., 10° for PCP and 45° for PCH). Although this concept seems reasonable at first sight, it cannot explain the short triplet lifetime of PCH, which is similar to that of acyclic alkenes such as styrene ($\tau_{T_1} = 22$ ns⁴). According to Dreiding models, a six-membered ring cannot reach a perpendicular twisted T_1 funnel geometry.

The question about the nature of an efficient T_1 -state deactivation pathway in alkenes is still not answered. Breaking of CC single bonds in the rings, yielding biradicals, can be excluded for the compounds considered here because of the low T_1 energies (between 50 and 60 kcal/mol for styrene derivatives compared to >80 kcal/mol dissociation energy for CC single bonds^{19,22}). Because of the central role of the double bond in the process, several reaction pathways which concentrate on this basic chromophore have been proposed: (i) the double bond twist coordinate,^{2,3,8,19} (ii) syn pyramidalization at the double bond,^{12,14,23} (iii) anti pyramidalization at the double bond,¹⁹ (iv) the C=C bond stretching coordinate⁴ and (v) a benzene-like 1,6-biradicaloid intermediate structure.²⁴ Our previous investigation of the potential energy surface for the double bond twist path (i) in the bicyclic alkene norbornene¹⁹ has shown that the surface of the T_1 state is very flat and that the molecule in this state is more flexible than previously thought. The syn pyramidalization (ii) of the vinylic hydrogens was found to be energetically unfavorable compared to anti pyramidalized (iii) twisted structures. Since bond stretching alone does not couple triplet and singlet states^{13,25,26} and furthermore results in very unfavorable vibrational overlaps,²⁷ the C=C stretching pathway (iv) is not considered explicitly. Mechanism v is also not examined here because it cannot explain the strong variations of ISC in the series of cyclic compounds (this argument can also be put forward against pathway iv).

We calculate T_1 and S_0 potential energy curves for twisting and anti pyramidalization at the double bond with quantum chemical *ab initio* and density functional theory (DFT) methods. Due to the size of the molecules only a one-dimensional consideration of the T_1-S_0 intersystem crossing is computationally feasible, which can, however, provide at least (semi)-quantitative information. In this context it should be pointed out that most of the measurements cited have been performed in solution where an upper limit for the T_1 -state lifetime on the order of milliseconds is expected due to collision-induced deactivation with the solvent molecules.

The determination of the most efficient $T_1 \rightarrow S_0$ ISC reaction pathway should provide a theoretical model which can achieve the following goals: (i) a semiquantitative prediction of the observed dependence of the T_1 -state lifetime with the ring size and (ii) an explanation of the the observed increase of the T_1 lifetime upon substitution of vinylic hydrogen by a phenyl group.

The relationship between the T_1 -state lifetime and the number of substituted vinylic hydrogen atoms has been examined in detail for acyclic alkenes, e.g., the phenyl substitution of stilbene ($\tau_{T_1}(\text{stilbene}) = 50$ ns, $\tau_{T_1}(\text{triphenylethylene}) = 100$ ns, and $\tau_{T_1}(\text{tetraphenylethylene}) = 175$ ns; for an overview see ref 2). Since norbornene ($\tau_{T_1}(\text{NOR}) = 250$ ns) and 2-phenylnorbornene ($\tau_{T_1}(\text{PNOR}) = 2000$ ns) are the only experimentally examined couple of unsubstituted and phenyl-substituted cyclic alkenes, we include them as well; this continues our previous study on norbornene.¹⁹

2. Theoretical Methods

The $T_1 \rightarrow S_0$ intersystem-crossing process is investigated along one-dimensional reaction coordinates while all remaining geometric variables are optimized. Two possible reaction pathways are investigated (see Figure 2): (i) The double bond twisting pathway has been calculated with the dihedral angle θ_1 between the vinylic carbon atoms and their two neighbors as reaction coordinate (for styrene the dihedral angle $\text{H}_1\text{C}_1\text{C}_2\text{C}_\alpha$ and a planar methylene group is used). (ii) The anti pyramidalization of the vinylic carbon atoms is described with

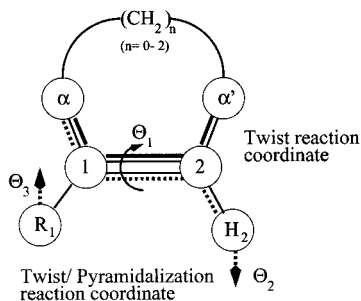


Figure 2. Definitions of reaction coordinates employed.

dihedral angles $\theta_2 = \angle(\text{H}_2\text{C}_2\text{C}_1\text{C}_\alpha) = \theta_3 = \angle(\text{R}_1\text{C}_1\text{C}_2\text{C}_\alpha)$. This coordinate contains components of pyramidalization as well as twisting and gives a local C_2 symmetry of the olefinic double bond. (iii) For the phenyl-substituted derivatives, we additionally investigate θ_2 as a reaction coordinate only and freely optimize θ_3 (nonsymmetrical antipyramidalization pathway). All geometry optimizations are carried out without any further symmetry constraints on the electronic or geometric structure using the eigenvector-following algorithm of Baker.²⁸

The geometries and energies have been calculated using unrestricted Kohn–Sham density functional theory (UDFT) with the B3LYP hybrid exchange–correlation functional.^{29,30} As found previously,¹⁹ the UDFT approach is quite robust against spin contamination of the wave functions so that the $\langle S^2 \rangle$ expectation values in most cases deviate by less than 0.01 from pure singlet or triplet multiplicity. Systematic investigations on the performance of the DFT/B3LYP approach for triplet states have not been performed yet, but comparisons with *ab initio* results for smaller systems^{31,32} suggest that this approach is quite useful for energetics and geometries. The TURBOMOLE^{33,34} suite of programs has been employed in all DFT calculations. The Gaussian basis sets used are of split-valence quality (SV, [3s2p]/[2s] for C and H, respectively),³⁵ subsequently augmented with polarization d functions at the carbon atoms ($\alpha_d = 0.8$, SV+d basis). Prior experience has shown that this theoretical level provides geometries and energies very similar to those of *ab initio* CASSCF and multireference singles and doubles configuration interaction (MRD-CI) calculations.¹⁹ To check the accuracy of the UDFT potential energy curves, we have performed MRD-CI calculations^{36,37} with the DIESEL-MR-CI program³⁸ for the S_0 and T_1 states of the unsubstituted compounds CB, CP, and CH. Harmonic vibrational frequencies for all stationary points are calculated at the UDFT-B3LYP/SV+d level with the GAUSSIAN 98 code.³⁹

In addition to the different reaction coordinates we examine the role of FCFs and SOC on the triplet-state lifetime. In our one-dimensional model, the transition rate (see eq 1) is proportional to the square of (isoenergetical) T_1 and S_0 vibrational wave functions weighted by the coordinate-dependent spin–orbit coupling matrix element. The density of states is assumed to be the same for all compounds and has been taken as the literature value of $\rho_{S_0} = 0.2786/\text{cm}^{-1}$ for ethene.⁷ The rates are calculated between (thermally populated) vibronic triplet state levels (v_i') ($i = 0, 1, 2, \dots$) and excited vibronic levels of the ground state (v_j). For convenience, the FCF values in the tables are reported for the lowest triplet v_0' level only. The vibrational wave functions are obtained by solving the one-dimensional Schrödinger equation numerically.⁴⁰ The reduced inertial moments for the twist and anti pyramidalization motions for each molecule are adjusted such that the one-dimensional (anharmonic) calculation yields the same fundamental frequency as the harmonic (multidimensional) calculation for the S_0 state. For the larger molecules there is some ambiguity in the

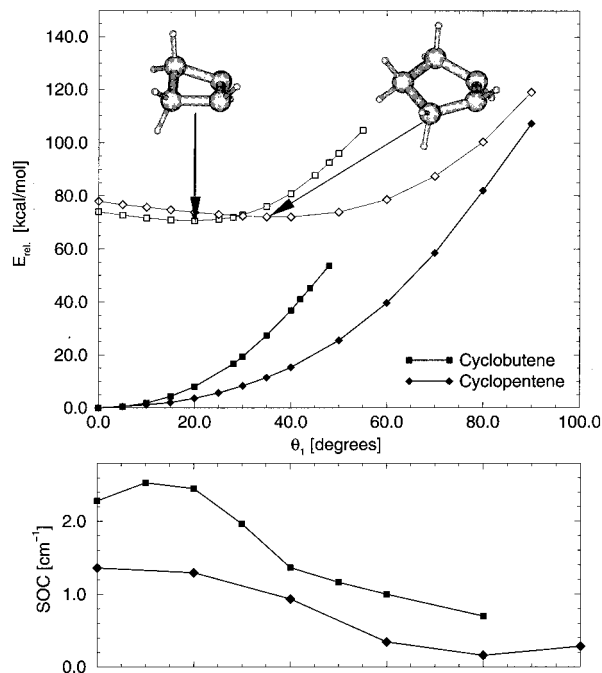


Figure 3. Potential energy curves (energies in kilocalories per mole relative to the minimum of the S_0 state) along the double bond twisting coordinate in cyclobutene and cyclopentene at the UDFT-B3LYP level. Open (filled) symbols correspond to triplet (singlet) states. Corresponding T_1 – S_0 spin–orbit matrix elements plotted along the same coordinate are shown in the lower figure.

assignment of the normal modes to either twisting or pyramidalization motions due to a strong mixing (generally 2–4 normal modes with twisting/pyramidalization character in the range 200–800 cm^{-1} are found). Test calculations using different reduced moments, however, give final results for the lifetimes within a deviation of 20%.

The calculations of the SOC constants are performed with the GAUSSIAN 98³⁹ package, which employs an approximate one-electron spin–orbit operator with an effective nuclear charge, $Z^* = 3.6$, determined previously by Koseki et al.^{41,42} The SOC calculations are carried out with CASSCF(2,2) wave functions (SV+d AO basis) employing the triplet-state geometry from UDFT calculations. Test calculations using CISDTQ(12,-12) wave functions carried out at selected geometries gave SOC values similar to those of the CASSCF(2,2) treatment.

The calculated $T_1 \rightarrow S_0$ decay rates which are equal to the inverse of T_1 -state lifetimes are weighed by the corresponding thermal population (Boltzman factor at $T = 300$ K) of the triplet-state levels. Because the rates are determined mainly by transitions from the (v_0') level, the thermally averaged values deviate by less than 10% from the zero temperature limit.

3. Results and Discussion

3.1. Twisting Coordinate. *3.1.1. Cyclobutene.* The S_0 state of cyclobutene is found to be planar with C_{2v} symmetry and a typical double bond length of 1.34 Å. Because of the four-membered ring, the strain energy is quite high (29 kcal/mol²¹). The minimum found for the T_1 state has about 20° of twist, much more than earlier expected.² The minimum is reached along the twisting coordinate without any barrier (see Figure 3). In the T_1 state, the C_1 – C_2 bond is strongly elongated to 1.50 Å and an anti pyramidalization of the hydrogen atoms at C_1 and C_2 ($\theta_{2/3} = -107^\circ$) is found. In the S_0 as well as in the T_1 state the whole molecule accommodates the forced twist by performing a C_2 -symmetrical butterfly-type structure with the

C_2 and C_α atoms remaining fixed and C_1 and $C_{\alpha'}$ moving symmetrically above the former molecular plane.

The potential energy curve of the S_0 state is well separated from that of the T_1 state along the entire path. In Figure 3, the dependence of SOC constants along the reaction coordinate is also presented. After a maximum SOC of 2.5 cm^{-1} at $\theta_1 = 10^\circ$ the values decrease monotonically to a minimum of 1.0 cm^{-1} at $\theta_1 = 70^\circ$.

3.1.2. Cyclopentene. The ground-state structure of cyclopentene has C_s symmetry with a ring-puckering angle $C_2C_\alpha C_\beta C_\alpha$ of 21.0° (exptl, 23.3° ¹⁴). The strain energy of the ground state has been calculated to be about 7 kcal/mol.¹⁷ A planar structure is about 0.5 kcal/mol less stable than the C_s -symmetric enveloped geometry,^{17,43} which demonstrates the increased flexibility of CP relative to CB. Although the potential energy curves shown in Figure 3 are quite similar to those of CB, we observe distinct differences due to released strain. The minimum of the T_1 state shifts to larger twist angles (about 35°), and a smaller anti pyramidalization of the hydrogen atoms at C_1 and C_2 ($\theta_2 = -109^\circ$) is found. The experimentally determined vertical triplet energy of 79 kcal/mol⁴ is in good agreement with the theoretical results (UDFT-B3LYP, 78.0 kcal/mol), demonstrating the reliability of the DFT approach. The shape of the SOC function resembles that of CB, but the values are generally about 1 cm^{-1} lower. Especially at energetically favorable geometries for ISC ($\theta_1 = 60\text{--}90^\circ$) the SOC values are found to be very small ($<0.5 \text{ cm}^{-1}$).

3.1.3. Cyclohexene. For the ground-state *cis*-isomer of CH two conformations have been published by Allinger and Sprague¹⁷ and Strickland and Caldwell.⁴⁴ Strickland and Caldwell investigated a half-chair and a half-boat structure, and in accordance with our results they found the half-chair to be the most stable structure.

Cyclohexene is the first alkene in our series for which a *trans*-isomer should be considered in addition to the *cis*-isomer. However, no experimental indications for the existence of *trans*-CH as a discrete chemical species have been reported to date, although Dauben et al.⁴⁵ proved the formation of *trans*-1-phenylcyclohexene upon flash pyrolysis of the *cis*-isomer. From molecular mechanics calculations, Allinger and Sprague¹⁷ predict the *trans*-isomer of CH to be 42 kcal/mol less stable than the *cis*-species. They could not find a transition state for the *trans* \rightarrow *cis* isomerization but estimated a barrier of about 13 kcal/mol. On the basis of MNDO calculations Maier and Schleyer⁴⁶ concluded that the *trans*-isomer does not exist. Verbeek⁴⁷ calculated C_2 -symmetrical structures of *cis*- and *trans*-isomers using GVB/STO-3G and MRD-CI/6-31G* methods and found a transition state which is 10 kcal/mol less stable than the *trans*-isomer. At the DFT level we find *trans*-CH to be a minimum with a lowest harmonic vibrational frequency of 269 cm^{-1} . The barrier, however, is less than $<1 \text{ kcal/mol}$ so that the existence of *trans*-CH as a discrete species is questionable. The DFT-B3LYP S_0 structure has a twist angle of 87.9° and strongly anti pyramidalized hydrogen atoms at C_1 and C_2 ($\theta_{2/3} = -43.9^\circ$) in agreement with the X-ray structure given by Dauben et al.⁴⁵ Isomerization energies have been theoretically studied using several force field, semiempirical, and *ab initio* methods due to missing experimental data:⁴⁴ MM3 provides 35.0 kcal/mol, AM1 59.4 kcal/mol, PM3 56.9 kcal/mol, and HF/6-31G 73.6 kcal/mol. From our DFT and MRD-CI calculations we obtain isomerization energies of 54.4 and 55.7 kcal/mol, respectively.

The calculated T_1 -state minimum of CH shows the expected large twist angle ($\theta_1 = 52.4^\circ$). The C_1 - C_2 bond is elongated

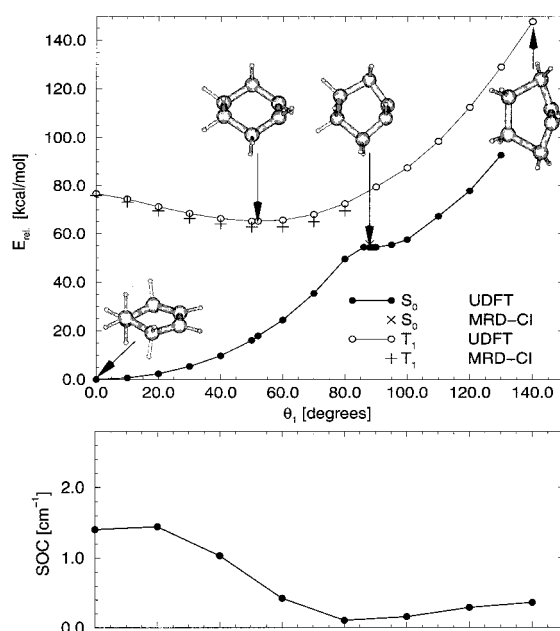


Figure 4. Potential energy curves (energies in kilocalories per mole relative to the minimum of the S_0 state) along the double bond twisting coordinate in cyclohexene at the UDFT-B3LYP and MRD-CI levels. The MRD-CI energies have been obtained in single-point calculations employing the UDFT geometries. Open (filled) symbols correspond to triplet (singlet) states. Corresponding T_1 - S_0 spin-orbit matrix elements plotted along the same coordinate are shown in the lower figure. The MRD-CI calculations for the S_0 state have been performed only at $\theta_1 = 0^\circ$ and 88° , respectively.

to 1.47 \AA , and the anti pyramidalization of the hydrogen atoms at C_1 and C_2 ($\theta_2 = -101^\circ$) decreases relative to that of the S_0 state. The potential energy curves are shown in Figure 4. Contrary to the S_0 curves computed for CB and CP, we observe a very flat region near 90° of twist, which corresponds to the *trans*-isomer. As for CB and CP we observe no barrier on the T_1 surface in going from the nontwisted structure to the minimum. The shape of the T_1 and S_0 potential curves can be interpreted as the sum of dumbbell curves for *cis*-*trans* isomerization and of a steeply rising curve due to ring strain for twist angles above 90° .^{3,48} The experimentally observed vertical triplet energy of 80.5 kcal/mol ⁴ is in reasonable agreement with our results (UDFT-B3LYP, 76.7 kcal/mol ; MRD-CI, 76.0 kcal/mol). To demonstrate the reliability of the DFT approach, we present a comparison of UDFT and MRD-CI energies in Figure 4. As found before for CB and CP the UDFT energies of the S_0 (only one value at 90° shown) and T_1 states are very close to those at the MRD-CI level even for twist angles $>60^\circ$ (where the S_0 state of ethene corresponds to a pure biradical). The functional dependence of the SOC values along the reaction coordinate is very similar to those of CP.

3.1.4. Phenylcycloalkenes. The potential energy curves for the S_0 and T_1 states and the T_1 minimum geometries of the phenylcycloalkenes and styrene are summarized in Figure 5. We have also included results for styrene in the figure, which shows the expected minimum (maximum) at a fully twisted geometry for the T_1 (S_0) state. There is no need for a detailed discussion of the individual compounds because of a very close resemblance of the potential energy curves to those of the unsubstituted molecules. Due to conjugative effects and some change of the biradicalic character from 1,2 to 1,6, the T_1 -state energies are generally lowered by about 15 kcal/mol compared to those of the unsubstituted systems. All T_1 -state potential curves show a minimum, and no barrier is found between $\theta_1 =$

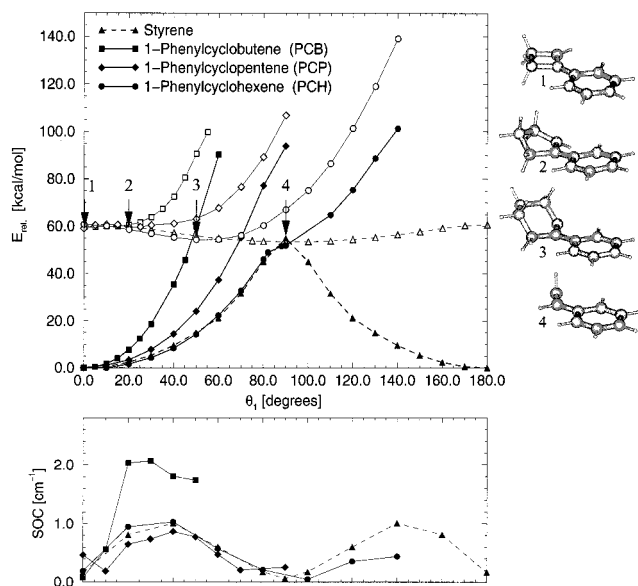


Figure 5. Potential energy curves (energies in kilocalories per mole relative to the minimum of the S_0 state) along the double bond twisting coordinate in the 1-phenylcycloalkenes and styrene at the UDFT/B3LYP level. Open (filled) symbols correspond to triplet (singlet) states. The optimized T_1 minimum geometries illustrate the increasing perpendicularity of the substituted methylene moieties with increasing ring size. Corresponding T_1 - S_0 spin-orbit matrix elements plotted along the same coordinate are shown in the lower figure.

0° and the minimum. Except for styrene, no crossing point with the S_0 state is found. The SOC constants increase with increasing twist angle to a maximum at about 45° and reach a minimum around 90° . The maximum SOC values are slightly lower compared to those of the corresponding unsubstituted compounds. Thus, our results confirm earlier conclusions based on calculations for ethene^{7,16} that SOC is very inefficient for geometries near the twisting funnel and even zero for a twisting angle of 90° . The T_1 -state geometries differ substantially from those of the unsubstituted alkenes: the styrene chromophore is distorted in a quinoid manner, and only the carbon atom C_2 pyramidalizes (see Figures 2 and 5). The amount of anti pyramidalization decreases in the series as $PCB > PCP > PCH$. This can be explained by the Coulomb repulsion between the two unpaired electrons in the triplet state which try to avoid each other. In the small ring compounds this is possible solely by pyramidalization while the large compounds have the ability to twist.

The T_1 states of the phenylalkenes are well studied experimentally.^{4,8,20,45,49} Ni et al.⁴ measured vertical ($E(T_1^v)$) and 0-0 triplet excitation ($E(T_1^e)$) energies for styrene, PCP, and PCH. For styrene we obtain $E(T_1^v) = 61.4$ kcal/mol and $E(T_1^e) = 54.2$ kcal/mol (experiment, 60.8 and 51.2 kcal/mol, respectively). For PCP Ni et al.⁴ find the T_1^e energy to be nearly identical to $E(T_1^v) = 59$ kcal/mol, which is in good agreement with the calculated data ($E(T_1^v) = 59.4$ kcal/mol, $E(T_1^e) = 59.1$ kcal/mol). For PCH the experimental data for the vertical ($E(T_1^v) = 60.8$ kcal/mol) and relaxed T_1 ($E(T_1^e) = 56.4$ kcal/mol) energies differ quite substantially, which is confirmed by the UDFT calculations ($E(T_1^v) = 60.8$ kcal/mol, $E(T_1^e) = 54.3$ kcal/mol). In agreement with Dauben et al.⁴⁵ we find a *trans* minimum structure for the S_0 state of PCH ($\theta_1 = 88.0^\circ$, $\theta_2 = -61.1^\circ$, $\theta_3 = -40.3^\circ$), a tiny barrier for *trans* \rightarrow *cis* isomerization, and an isomerization energy of 51.7 kcal/mol (experiment, 47.0 kcal/mol⁴⁴).

TABLE 1: Excitation Energies and Dihedral Angles θ (for Definitions, See Figure 2) for the T_1 State of the Investigated Olefines

compd	$E(T_1)$ (vert/min) (kcal/mol)	$E(T_1)$ (exptl) (vert/min) (kcal/mol)	θ_1 (deg)	$\theta_{2/3}$ (deg)
CB	74.0/70.7	—/—	20.0	-106.7/-106.7 ^a
CP	77.9/72.1	79.4 ⁴ /—	35.0	-109.2/-109.2 ^a
CH	76.7/65.2	80.5 ⁴ /—	52.0	-101.6/-101.6 ^a
NOR	73.0/68.7	72.3 ¹⁸ /60.6 ¹⁸	11.8	-121.3/-128.2
PCB	59.5/59.5	—/—	0.0	-179.5/-179.9
PCP	59.4/59.1	59.2 ⁴ /58.9 ⁴	20.0	-155.3/-142.6
PCH	60.8/54.3	60.8 ⁴ /56.4 ⁴	50.0	-126.1/-102.1
STYR	61.4/54.2	60.8 ²⁴ /51.2 ²⁴	90.0	-89.1/-93.4

^aThe structures have C_2 symmetry.

TABLE 2: Franck-Condon Factors, Fundamental Vibrational Frequencies ω , and Calculated and Experimental T_1 -State Lifetimes for the Double Bond Twisting Reaction Path

compd	ω_{S_0} (cm^{-1})	ω_{T_1} (cm^{-1})	FCF	τ_{T_1} (calcd) (s)	τ_{T_1} (exptl) (s)
CB	398.2	345.5	2.96×10^{-10}	2.95	
CP	395.5	344.2	1.46×10^{-8}	2.07	
CH	398.1	444.9	1.31×10^{-9}	2.32	
NOR	477.4	598.7	3.50×10^{-11}	9.00×10^{-2}	2.50×10^{-7} ¹⁸
PCB	242.7	115.0	2.25×10^{-12}	1.34	3.60×10^{-3} ⁸
PCP	257.4	6.6	4.23×10^{-11}	7.00×10^{-2}	1.50×10^{-5} ⁴
PCH	257.4	361.0	3.82×10^{-11}	8.00×10^{-2}	5.60×10^{-8} ⁴
STYR	1026.7	386.1	5.24×10^{-4}	5.78×10^{-9}	2.20×10^{-8} ⁴

3.1.5. Discussion. The most important data characterizing the T_1 -state geometries along the double bond twist reaction pathway for the investigated alkenes are summarized in Table 1.

First of all we notice a very good agreement between theory and experiment for the excitation energies. The increased ability of the larger rings to twist is documented by an increased θ_1 value for the T_1 -state minimum, thereby reducing the energy gap relative to that of the S_0 state. The θ_1 value for the bicyclic compound norbornene is even smaller (12°) than that of CB (20°). The phenyl-substituted carbon rings tend to be less flexible (i.e., have lower θ_1 values), which can be explained by the conjugation of the benzene ring with the double bond. Thus, PCB is planar in the T_1 state while PCP and PCH show significant anti pyramidalization of the vinylic hydrogen atoms in addition to the double bond twist. Qualitatively, the shape of the potential curves seems to be in line with the free-rotor model.

The calculated SOC constants show no trend with respect to ring size and thus cannot explain the different ISC efficiencies. According to Siebrand⁹ the FCFs control the intersystem-crossing rates if the SOC constants are small ($< 1 \text{ cm}^{-1}$). To check this hypothesis, one-dimensional FCFs as the square of the overlap between isoenergetical lying vibrational wave functions are calculated and are given in Table 2. In addition, the fundamental vibrational frequencies ω_{S_0} and ω_{T_1} and calculated and experimental T_1 -state lifetimes are discussed.

The vibrational states for the S_0 states become isoenergetic with the lowest level of the T_1 state for vibrational quantum numbers between 60 and 80 in the different molecules. Except for styrene, all FCF values are below 10^{-8} . As a result, the thermally averaged T_1 -state lifetimes are very long, i.e., reaching seconds for the unsubstituted compounds and PCB and milliseconds for NOR, PCP, and PCH. Furthermore, neither the FCF values nor the calculated lifetimes reflect the observed trend

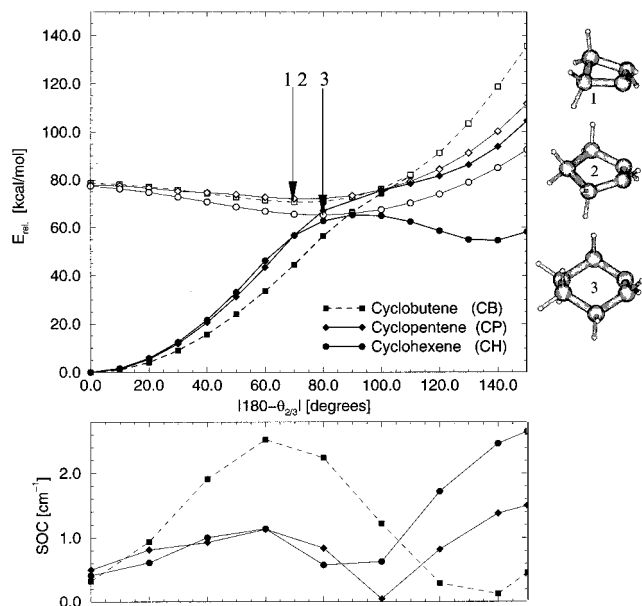


Figure 6. Potential energy curves (energies in kilocalories per mole relative to the minimum of the S_0 state) along the symmetrical anti pyramidalization coordinate ($\theta_2 = \theta_3$) of cyclobutene, cyclopentene, and cyclohexene and at the UDFT-B3LYP level. Open (filled) symbols correspond to triplet (singlet) states. The arrows indicate the position of the triplet-state geometries shown. Corresponding T_1 - S_0 spin-orbit matrix elements plotted along the same coordinate are shown in the lower figure.

with ring size. Only for styrene, which is not hindered in the ability to twist, we find good agreement between theory and experiment (6 and 22 ns, respectively) [the good agreement on an absolute time scale is fortuitous due to compensating errors in the assumed density of states (too low) and the FCFs for the neglected modes (which are not unity)]. The calculated data for this compound ($SOC = 0.03 \text{ cm}^{-1}$ at $\theta_1 = 90^\circ$, $FCF = 5.24 \times 10^{-4}$) indicate a FC-controlled ISC mechanism. Because of the striking disagreement of the theoretical predictions with the experimental observations for the cyclic compounds, we conclude that a pure double bond twist reaction path is not responsible for the ISC. The main reason for this behavior is the absence of a crossing or touching point between the T_1 and S_0 potential curves.

There is theoretical and experimental evidence that additional motions other than twist play an important role in the ISC process. All T_1 minimum geometries for the twist reaction coordinate as well as the X-ray structure of *trans*-PCH show large anti pyramidalization at the double bond. Substitution of these vinylic hydrogen atoms is experimentally known² to have a large influence on the T_1 -state lifetime. Furthermore, SOC increases for ethene by pyramidalization at the carbon atoms.¹⁶ Thus, we investigate an anti pyramidalization coordinate which contains components of both anti pyramidalization and twist. This coordinate closely resembles the normal modes of the molecules in the 200–800 cm^{-1} range which are of mixed twist/anti pyramidalization character.

3.2. Anti Pyramidalization Coordinate. **3.2.1. Cyclobutene, Cyclopentene, and Cyclohexene.** The potential energy curves for the S_0 and T_1 states along the C_2 -symmetrical anti pyramidalization coordinate θ_2 for CB, CP, and CH are shown in Figure 6. The potential curves differ substantially from those along the pure double bond twist reaction coordinate. Note that the minima in S_0 and T_1 correspond to those shown for the twist coordinate; i.e., the multidimensional surfaces are now explored from the minima along another direction.

The energy of the S_0 state increases more strongly compared to the twist coordinate, and the ordering of the steepness for the different compounds is reversed (i.e., $CH > CP > CB$). The potential energy curves for the T_1 state are extremely flat; i.e., the energy increases by less than 5–10 kcal/mol from the minimum to either 0° or 100° . All S_0 curves touch the T_1 -state curve in the region of the T_1 minimum (CB at $\theta_2 = 110^\circ$, CP at $\theta_2 = 100^\circ$, and CH at $\theta_2 = 90^\circ$), and it seems that the anti pyramidalization pathway provides a funnel for ISC much more effectively than the twisting coordinate. As expected, the position of the touching point moves toward the minimum with decreasing rigidity of the ring. The potential curve for the S_0 state of CH shows a second minimum at about $\theta_2 = 135^\circ$ corresponding to the *trans*-isomer.

In Figure 6 we also present the SOC constants along this coordinate. Starting with small SOC values at $\theta_2 = 0^\circ$, they increase to a maximum at 60° , i.e., near the T_1 minima (CB, 2.6 cm^{-1} ; CP, 1.1 cm^{-1} ; CH, 1.1 cm^{-1}). Although the SOC values decrease for larger values of the reaction coordinate, nevertheless the SOC values near the anti pyramidalized T_1 state minimum geometries are definitely higher ($>0.5 \text{ cm}^{-1}$) compared to corresponding points on the twist reaction path. These findings, together with large FCF due to touching of the curves near the T_1 minimum, explain the extremely short lifetimes ($<1 \text{ ns}$) calculated for CB and CP. A similar value may also be expected for CH but could not be calculated in our model because of the appearance of the second minimum on the T_1 surface.

3.2.2. Phenylcycloalkenes. First, we investigated the T_1 and S_0 potential energy curves along the anti pyramidalization/twist coordinate in the same manner as for the unsubstituted cyclic alkenes ($\theta_2 = \theta_3$, i.e., local C_2 symmetry). The calculated triplet and singlet potential curves (not shown) resemble those of the unsubstituted parent molecules with extreme flat but more repulsive triplet curves. The T_1 - S_0 crossing points were also found at similar θ_2 values (PCB, $\theta_2 = 78^\circ$; PCP, $\theta_2 = 70^\circ$; PCH, $\theta_2 = 62^\circ$). The T_1 minima, however, were always found at $\theta_{2/3} = 0^\circ$. Because the minima of the T_1 and S_0 states are located exactly above each other and the potentials are quite harmonic, we calculate very low FCF values of $<10^{-10}$. Furthermore, the trend of the FCF (e.g., PCP $>$ PCH) does not reflect the observed trend of the ISC efficiencies. Thus, we can conclude that the ISC reaction on this coordinate seems to be very inefficient for the phenyl-substituted compounds while it is the most reliable pathway for the unsubstituted systems. This difference can be traced back to the conjugation between the benzene ring and the double bond, which further increases in the T_1 state. Increasing $\theta_{2/3}$ results in a loss of conjugative interaction and thus in energetically very unfavorable situations at larger values for the reaction coordinate.

Therefore, we investigate the T_1 and S_0 potential curves along the reaction coordinate θ_3 alone, which yields a nonsymmetrical anti pyramidalization at the carbon atom C_2 (see Figure 7 and Table 3). These potential curves show a slightly different shape along positive and negative directions due to the unsymmetrical arrangement of the pyramidalizing hydrogen atom with respect to the two rings.

The shape of the T_1 and S_0 potential curves for PCB is very similar to that of the symmetrical situation, i.e., a T_1 minimum at 0° and no crossing point. The FCF values are only slightly larger compared to the pure twist coordinate ($FCF(\text{twist}) = 2.25 \times 10^{-12}$, $FCF(\text{anti pyramidalization}) = 8.01 \times 10^{-11}$). The higher SOC values explain the decrease of the calculated T_1 -

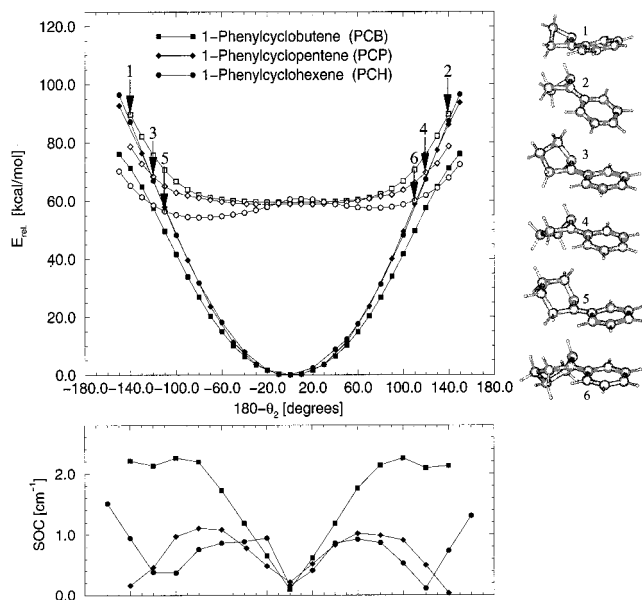


Figure 7. Potential energy curves (energies in kilocalories per mole relative to the minimum of the S_0 state) along the anti pyramidalization coordinate ($\theta_2 \neq \theta_3$) of 1-phenylcyclobutene, 1-phenylcyclopentene, and 1-phenylcyclohexene. Open (filled) symbols correspond to triplet (singlet) states. The arrows indicate the position of the triplet-state geometries shown. Corresponding T_1 – S_0 spin–orbit matrix elements plotted along the same coordinate are shown in the lower figure.

TABLE 3: Franck–Condon Factors, Fundamental Vibrational Frequencies ω , and Calculated and Experimental T_1 -State Lifetimes for the Combined Twist/Anti Pyramidalization Pathway

compd	ω_{S_0} (cm^{-1})	ω_{T_1} (cm^{-1})	FCF	$\tau_{T_1}(\text{calcd})$ (s)	$\tau_{T_1}(\text{exptl})$ (s)
$\theta_2 = \theta_3$ Pathway with Local C_2 Symmetry					
CB	946.2	651.4	2.25×10^{-2}	1.35×10^{-10}	
CP	977.8	539.7	6.63×10^{-2}	4.58×10^{-11}	
CH	1002.1	565.2	<i>a</i>	<i>a</i>	
NOR	900.7	569.3	1.04×10^{-3}	2.93×10^{-9}	2.50×10^{-7} ¹⁸
$\theta_2 \neq \theta_3$ Pathway					
PCB	884.7	267.3	8.01×10^{-11}	4.00×10^{-2}	3.60×10^{-3} ¹⁸
PCP	841.0	206.3	8.12×10^{-8}	3.75×10^{-5}	1.50×10^{-5} ⁴
PCH	879.0	464.6	4.80×10^{-4}	6.36×10^{-9}	5.60×10^{-8} ⁴
PNOR	870.4	277.0	2.64×10^{-8}	1.15×10^{-4}	$\geq 2.00 \times 10^{-6}$ ⁵

^aDue to the second minimum on the S_0 surface, no isoenergetically lying vibrational wave functions for the T_1 and S_0 states can be found.

state lifetime from 1.34 s for the twist path to 40 ms. This result is in reasonable agreement with the experimental lifetime of 3.6 ms.⁸

The S_0 potential curve of PCP is slightly steeper compared to that of PCB, and we find a very shallow minimum of 0.1 kcal/mol depth at $\theta_2 = -50^\circ$ for the T_1 state. As a result we calculate a FCF value 3 orders of magnitude larger than that of PCB. The calculated lifetime of 37.5 μs is in good agreement with the experimental value of about 15 μs .⁸

The trend in the shape of the T_1 -state potential curves continues for PCH. The curve has deeper minima which are moved to larger values of the reaction coordinate ($|\theta_2| \approx 90^\circ$), which is quite close to the T_1 – S_0 crossing points at $|\theta_2| \approx 110^\circ$. The FCF value increases by 4 orders of magnitude compared to that of PCP, and the calculated lifetime decreases to 6.4 ns. Again, this theoretical result is in reasonable agreement with the experimental value of about 56 ns.⁸

In summary we can conclude that this pathway not only provides the correct trend for the ISC efficiencies for the three

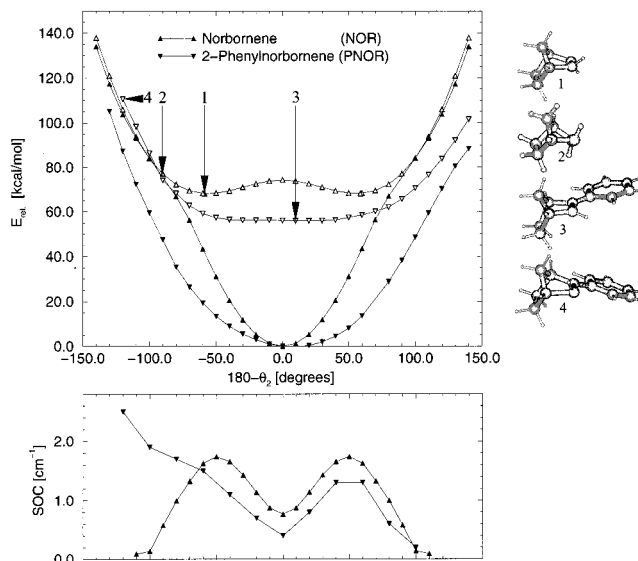


Figure 8. Potential energy curves (energies in kilocalories per mole relative to the minimum of the S_0 state) along the anti-pyramidalization coordinate ($\theta_2 \neq \theta_3$) of norbornene and 2-phenylnorbornene. Open (filled) symbols correspond to triplet (singlet) states. Corresponding T_1 – S_0 spin–orbit matrix elements plotted along the same coordinate are shown in the lower figure.

compounds but also gives a surprisingly good agreement between theory and experiment for the lifetime shortening with ring size.

3.2.3. Norbornene and 2-Phenylnorbornene. The calculated T_1 -state lifetimes for the unsubstituted alkenes (see Table 3) are significantly shorter than for the phenyl-substituted derivatives. From experiments done with phenyl-substituted ethenes (for details see ref 2) it has been supposed that the replacement of hydrogen at the double bond by an organic group increases the T_1 -state lifetime monotonically. The only experimental data for a pair of cyclic alkenes are available for norbornene and 2-phenylnorbornene (PNOR). The simulation of this effect may serve as a further test for the validity of our theoretical model. The calculated T_1 and S_0 potential curves and SOC constants for the two bicyclic alkenes are presented in Figure 8.

For both compounds the T_1 and S_0 potential energy curves resemble those of CP and PCP, respectively. For NOR, the S_0 -state potential curve is slightly steeper than for CP, and therefore the S_0 curve crosses the T_1 state at larger values of the reaction coordinate ($\theta_2 = 96^\circ$). The T_1 potential curve of NOR is extremely flat and shifted by about 3 kcal/mol to lower T_1 -state energies compared to that of CP. The calculated excitation energy $E(T_1^v)$ of NOR ($E(T_1^v) = 74.4$ kcal/mol) is in good agreement with the experimental value of 72.3 kcal/mol.¹⁸ Because the SOC values for NOR and CP are very similar and the potential curves of NOR result in a lower FCF (CP, 6.63×10^{-2} ; NOR, 1.04×10^{-3}), we arrive at a longer calculated T_1 -state lifetime of about 2.9 ns (CP, 0.05 ns), which is in qualitative agreement with the short experimental lifetime of 250 ns.¹⁸ This result confirms our previous conclusion¹⁹ that the lifetime of NOR cannot be explained within a twist-only mechanism. The comparison with CP clearly shows that the increased calculated lifetime for NOR results from a higher rigidity of the bicyclic compared to the monocyclic ring system.

For PNOR, which behaves in all respects very similar to PCP, we calculate a T_1 -state lifetime of about 130 μs , which is not too far away from the experimental estimation of > 2 μs . Thus, our approach is also able to reproduce at least semiquantitatively the observed substituent effect (increased T_1 -state lifetime due

to phenyl substitution). The main reason for this is, as for the other pairs of compounds, the stronger preference of the phenylalkenes for a planar T_1 -state geometry.

4. Conclusions

We have investigated the lowest singlet (S_0) and triplet (T_1) state potential energy surfaces for distortions of the double bond of the cyclic alkenes C_nH_{2n-2} ($n = 4, 5, 6$), their 1-phenyl-substituted derivatives, norbornene, and 1-phenylnorbornene, and styrene. UDFT calculations and *ab initio* MRD-CI methods provide very similar results for different structures and states. The vertical and adiabatic excitation energies from the UDFT treatments are in good agreement (errors $<2-3$ kcal/mol) with the experimental data.

In agreement with predictions of the simple free-rotor model, the released strain in larger cycloalkenes results in a larger ability to twist. The small FCFs and energetically unfavorable lying crossing points between S_0 and T_1 surfaces, however, exclude this pathway for an explanation of the efficient ISC in the alkenes. The anti pyramidalization of the vinylic hydrogens combined with a double bond twisting provides a low-energy pathway which leads to a T_1-S_0 surface crossing or touching near the minimum of the T_1 state for all compounds studied. The calculated FCFs for this pathway are at least 6 (cycloalkenes) or 3 (phenylcycloalkenes) magnitudes larger than for the twisting coordinate. Although the computed SOCs near the T_1-S_0 crossing points decrease with increasing ring size, our calculations correctly predict a proportionality between the $T_1 \rightarrow S_0$ ISC efficiency and the ring size. Furthermore, our one-dimensional model (which is the basic approximation used) also yields a very good agreement between calculated and experimental T_1 -state lifetimes.

In conclusion we can say that the free-rotor model gives the right answer for the wrong reason: the twisting motion (on which the model was based) alone cannot explain the observed trends. Only together with the pyramidalization at the double bond carbon atoms, which becomes easier for the larger rings (as also for the twist), can reliable theoretical results be obtained. The experimentally observed influence of vinylic hydrogen substitution by phenyl groups (increasing T_1 -state lifetime) could also be reproduced. The reason for this can again be traced back to a change of the potential curves induced by a preferred planarity of the T_1 state in the phenyl-substituted compounds (conjugation effect). Siebrands rule⁹ that the ISC is dominated by the FCF if the SOC is weak is fully confirmed by our calculations.

Acknowledgment. This research is supported by a grant (I-461-230.5/95) from the GIF (German-Israeli Foundation). The services and computer time made available by the Sonderforschungsbereich 334 ("Wechselwirkungen in Molekülen") have been essential to this study. M.W. thanks M. Waletzke (Theoretische Chemie, Bonn) and Prof. Dr. M. Peric (Belgrade) for helpful discussions.

References and Notes

- (1) Turro, N. J. *Modern Molecular Photochemistry*; Benjamin Cummings: Menlo Park, CA, 1978.
- (2) Caldwell, R. A.; Cao, C. V. *J. Am. Chem. Soc.* **1982**, *104*, 6174.
- (3) Bonneau, R. *J. Photochem.* **1979**, *10*, 439.
- (4) Ni, T.; Caldwell, R. A.; Melton, L. A. *J. Am. Chem. Soc.* **1989**, *111*, 457.
- (5) Bonneau, R. *J. Am. Chem. Soc.* **1982**, *104*, 2921.
- (6) Buenker, R. J.; Peyerimhoff, S. D.; Hsu, H. L. *Chem. Phys. Lett.* **1971**, *11*, 65.
- (7) Gemein, B.; Peyerimhoff, S. D. *J. Phys. Chem.* **1996**, *100*, 19257.
- (8) Zimmerman, H. E.; Kamm, K. S.; Werthemann, D. P. *J. Am. Chem. Soc.* **1975**, *97*, 3718.
- (9) Siebrand, W. J. *J. Chem. Phys.* **1967**, *46*, 440.
- (10) Klessinger, M.; Michl, J. *Excited States and Photochemistry of Organic Molecules*; Verlag Chemie: Weinheim, Germany, 1995.
- (11) Salem, L.; Rowland, C. *Angew. Chem., Int. Ed. Engl.* **1972**, *11*, 92.
- (12) Caldwell, R. A.; Caracci, L.; Doubleday, C. E.; Furlani, T. R.; King, H. F.; McIver, J. W. *J. Am. Chem. Soc.* **1988**, *110*, 6901.
- (13) Shaik, S. *J. Am. Chem. Soc.* **1979**, *101*, 2736.
- (14) Walsh, A. D. *J. Chem. Soc.* **1953**, 2325.
- (15) Ben-Nun, M.; Martinez, T. J. *Chem. Phys. Lett.* **1998**, *298*, 57.
- (16) Danovich, D.; Marian, C. M.; Neuheuser, T.; Peyerimhoff, S. D.; Shaik, S. *J. Phys. Chem. A* **1998**, *102*, 5923.
- (17) Allinger, N. L.; Sprague, J. T. *J. Am. Chem. Soc.* **1972**, *94*, 5734.
- (18) Barwise, A. J. G.; Gorman, A. A.; Rodgers, M. A. *J. Chem. Phys. Lett.* **1976**, *38*, 313.
- (19) Grimme, S.; Woeller, M.; Peyerimhoff, S. D.; Dannovich, D.; Shaik, S. *Chem. Phys. Lett.* **1998**, *287*, 601.
- (20) Goodman, J. L.; Peters, K. S.; Misawa, H.; Caldwell, R. A. *J. Am. Chem. Soc.* **1986**, *108*, 6103.
- (21) Grimme, S. *J. Am. Chem. Soc.* **1996**, *118*, 1533.
- (22) Vollhardt, K. P. C. *Organic Chemistry*; W. H. Freeman and Co.: New York and Oxford, 1987.
- (23) Arnold, D. R.; Abraitys, V. Y. *Mol. Photochem.* **1970**, *2*, 27.
- (24) Bearpark, M. J.; Olivucci, M.; Wilsey, S.; Bernardi, F.; Robb, M. A. *J. Am. Chem. Soc.* **1995**, *117*, 6944.
- (25) Shaik, S.; Epiotis, N. D. *J. Am. Chem. Soc.* **1978**, *100*, 18.
- (26) Shaik, S. *J. Am. Chem. Soc.* **1979**, *101*, 3184.
- (27) Grimme, S.; Woeller, M. Unpublished results.
- (28) Baker, J. J. *Comput. Chem.* **1986**, *7*, 385.
- (29) Becke, A. D. *J. Chem. Phys.* **1993**, *98*, 5648.
- (30) Stephens, P. J.; Devlin, F. J.; Chabalowski, C. F.; Frisch, M. J. *J. Phys. Chem.* **1994**, *98*, 11623.
- (31) Das, D.; Whittenburg, S. L. *J. Mol. Struct.* **1999**, *492*, 175.
- (32) Sumathi, R.; Hendrickx, M. *Chem. Phys. Lett.* **1998**, *287*, 496.
- (33) Ahlrichs, R.; Bär, M.; Häser, M.; Horn, H.; Kölmel, C. *Chem. Phys. Lett.* **1989**, *162*, 165.
- (34) Ahlrichs, R.; Treutler, O. *J. Chem. Phys.* **1995**, *102*, 346.
- (35) Ahlrichs, R.; Schäfer, A.; Horn, H. *J. Chem. Phys.* **1992**, *97*, 2571.
- (36) Peyerimhoff, S. D.; Buenker, R. J. *Theor. Chim. Acta* **1974**, *35*, 33.
- (37) Peyerimhoff, S. D.; Buenker, R. J. *Theor. Chim. Acta* **1975**, *39*, 217.
- (38) Hanrath, M.; Engels, B. *Chem. Phys.* **1997**, *225*, 197.
- (39) Frisch, M. J.; Trucks, G. W.; Schlegel, H. B.; Scuseria, G. E.; Robb, M. A.; Cheeseman, J. R.; Zakrzewski, V. G.; Montgomery, J. A.; Stratmann, R. E.; Burant, J. C.; Dapprich, S.; Millam, J. M.; Daniels, A. D.; Kudin, K. N.; Strain, M. C.; Farkas, O.; Tomasi, J.; Barone, V.; Cossi, M.; Cammi, R.; Mennucci, B.; Pomelli, C.; Adamo, C.; Clifford, S.; Ochterski, J.; Petersson, G. A.; Ayala, P. Y.; Cui, Q.; Morokuma, K.; Malick, D. K.; Rabuck, A. D.; Raghavachari, K.; Foresman, J. B.; Cioslowski, J.; Ortiz, J. V.; Baboul, A. G.; Stefanov, B. B.; Liu, G.; Liashenko, A.; Piskorz, P.; Komaromi, I.; Gomperts, R.; Martin, R. L.; Fox, D. J.; Keith, T.; Al-Laham, M. A.; Peng, C. Y.; Nanayakkara, A.; Gonzalez, C.; Challacombe, M.; Gill, P. M. W.; Johnson, B.; Chen, W.; Wong, M. W.; Andres, J. L.; Gonzalez, C.; Head-Gordon, M.; Replogle, E. S.; Pople, J. A. *Gaussian 98*, Rev. A7; Gaussian Inc.: Pittsburgh, PA, 1998.
- (40) Johnson, B. R. *J. Chem. Phys.* **1977**, *67*, 4086.
- (41) Gordon, M. S.; Koseki, S.; Schmidt, M. W. *J. Phys. Chem.* **1992**, *96*, 10768.
- (42) Koseki, S.; Gordon, M. S.; Schmidt, M. W.; Matsunaga, N. *J. Phys. Chem.* **1995**, *99*, 12764.
- (43) Mathies, R. A.; Lawless, M. K.; Wickham, S. W. *J. Am. Chem. Soc.* **1994**, *116*, 1593.
- (44) Strickland, A. D.; Caldwell, R. A. *J. Phys. Chem.* **1993**, *97*, 13394.
- (45) Dauben, W. G.; Riel, H. C. H. A. v.; Leroy, F.; Jousset-Dubien, J.; Bonneau, R. *J. Am. Chem. Soc.* **1980**, *101*, 1901.
- (46) Maier, W. F.; Schleyer, P. v. R. Presented at the 5th IUPAC Conference on Physical Organic Chemistry, Santa Cruz, CA, 1980.
- (47) Verbeek, J.; van Lenthe, J. H.; Timmermans, P. J.; Mackor, A.; Budzelaar, P. H. *J. Org. Chem.* **1987**, *52*, 2955.
- (48) Bonneau, R.; Jousset-Dubien, J.; Salem, L.; Yarwood, A. J. *J. Am. Chem. Soc.* **1976**, *98*, 4329.
- (49) Rondan, N. G.; Paddon-Row, M. N.; Caramella, P.; Houk, K. N. *J. Am. Chem. Soc.* **1981**, *103*, 2436.